Structure of Hydrated Na−Nafion Polymer Membranes

Nick P. Blake,[†] Matt K. Petersen,[‡] Gregory A. Voth,[‡] and Horia Metiu*[,†]

Department of Chemistry & Biochemistry, University of California, Santa Barbara, California 93106, and Department of Chemistry and Center for Biophysical Modeling and Simulation, University of Utah, Salt Lake City, Utah 84112

Received: August 19, 2005; In Final Form: October 24, 2005

We use molecular dynamics simulations to investigate the structure of the hydrated Na−Nafion membranes. The membrane is "prepared" by starting with the Nafion chains placed on a cylinder having the water inside it. Minimizing the energy of the system leads to a filamentary hydrophilic domain whose structure depends on the degree of hydration. At 5 wt % water the system does not have enough water molecules to solvate all the ions that could be formed by the dissociation of the $-SO_3Na$ groups. As a result, the $-SO_3Na$ groups aggregate with the water to form very small droplets that do not join into a continuous phase. The size of the droplets is between 5 and 8 Å. As the amount of water present in the membrane is increased, the membrane swells, and SO_3Na has an increasing tendency to dissociate into ions. Furthermore, a transition to a percolating hydrophilic network is observed. In the percolating structure, the water forms irregular curvilinear channels branching in all directions. The typical dimension of the cross section of these channels is about 10−20 Å. Calculated neutron scattering from the simulated system is in qualitative agreement with experiment. In all simulations, the pendant sulfonated perfluorovinyl side chains of the Nafion hug the walls of the hydrophilic channel, while the sulfonate groups point toward the center of the hydrophilic phase. The expulsion of the side chains from the hydrophilic domain is favored because it allows better interaction between the water molecules. We have also examined the probability of finding water molecules around the Na^+ and the $-SO_3^-$ ions as well as the probability of finding other water molecules next to a given water molecule. These probabilities are much broader than those found in bulk water or for one ion in bulk water (calculated with the potentials used in the present simulation). This is due to the highly inhomogeneous nature of the material contained in the small hydrophilic pores.

I. Introduction

Nafion is a poly(tetrafluoroethylene) (PTFE) polymer with hydrophilic perfluorovinyl pendant side chains terminated with sulfonic acid groups, used as a proton-conducting membrane in methanol or oxygen−hydrogen fuel cells. The PTFE backbone ensures long-term chemical stability in both reducing and oxidizing environments. The sulfonic headgroups on the side chains have very high acidity due to the presence of the electron-withdrawing $-CF_2-$ groups.

Nafion absorbs water and separates into domains of hydrophilic and hydrophobic phases, and ion conductivity takes place through the hydrophilic channels. An improved understanding of the morphology of these channels and the properties of the material in them may help improve fuel cell membranes. These hydrophilic domains are also scientifically intriguing. They are small in cross section, and the ion concentration in them is extremely high. As a result, the spatial confinement and the high ion concentration are likely to force this mixture of ions and water into an unusual structure.

Unfortunately, it is very difficult to obtain detailed experimental information about the morphology and the properties of these channels.[1] For this reason, atomic level simulations[1−15] are a valuable complement to the experiment.

Here we use molecular dynamics simulations to examine the structure of the material inside the hydrophilic domains and the manner in which this changes with the degree of hydration. Since dealing with protons requires a quantum mechanical treatment,[16] we concentrate here on the sodium salt of Nafion (which we call Na−Nafion). Such salts are of interest in themselves and have been characterized experimentally.

As we shall show, the tortuosity and inhomogeneity of the hydrophilic domains makes it difficult to characterize quantitatively the properties of the material inside them. Molecules near the surface of a domain have different properties than those in the middle. Moreover, water molecules away from an ion, near an ion, or between two ions are likely to differ from each other. These details, arising from inhomogeneity, are "washed out" in quantities used to characterize the structure of homogeneous fluids. Because of this, we express some of the structural properties of the fluid inside the hydrophilic domains by using histograms characterizing the size, and the connectivity, of water clusters, the number of water molecules or headgroups in the neighborhood of a Na ion, or the number of Na ions and water molecules in the proximity of a SO_3 headgroup.

A number of findings are worth mentioning here.

1. The side chains tend to line up along the domain wall, with the SO_3 group sticking out into the hydrophilic domain.

2. At low hydration levels, ion−ion interactions favor the formation of a series of narrow, winding, irregular clusters and isolated droplets—that may connect to one another via temporary water bridges. The $NaSO_3$ groups do not dissociate, and sodium has a tendency to coordinate with several SO_3 groups. The little water that is present prefers to solvate sodium; because of this,

[†] University of California, Santa Barbara.
[‡] University of Utah.

10.1021/jp054687r CCC: $30.25
Published on Web 12/06/2005

the number of water molecules in the neighborhood of a given water molecule is smaller than that seen in the bulk water.

3. At higher water loading, the water solvates the ions more effectively and screens the ion−ion interactions. The hydrophilic pore swells, and some SO_3Na dissociation is evident, with the SO_3^- groups located near the domain wall and the Na^+ ion moving toward the center of the hydrophilic channel. When the hydration exceeds 5 wt % water (roughly 30% relative humidity[21]), droplets give way to channel formation. A percolating network of water become evident, ultimately leading to a material with aqueous channels of high tortuosity that are 10−15 Å in diameter. At high levels of hydration (19 wt % water, ∼100% relative humidity[21]) the average water−water coordination is similar and occasionally exceeds that in bulk water.

II. The Model

Nafion is a polymer with the formula

$$\begin{array}{l} \text{...-}[(CF_2\text{-}CF_2)_n\text{-}CF\text{-}CF_2]_p\text{- ....} \\ \qquad\qquad\quad | \\ \qquad\quad (OCF_2\text{-}CF)_m\text{-}OCF_2CF_2\text{-}SO_3^-M^+ \\ \qquad\qquad\quad | \\ \qquad\qquad CF_3 \end{array} \qquad (1)$$

In a typical membrane $m = 1$, n varies between 5 and 14 and p varies between 200 and 1000. In our calculations we have used a cell that contains 8−12 Nafion strands having $p = 6$ and $n = 8$, with the hydration levels encountered in a typical membrane. Periodic boundary conditions simulate the fact that the membrane is "infinite". The cation M is Na.

The literature uses a specialized nomenclature to describe the structure of the polymer. The ratio of polar to nonpolar material in the membrane, determined by the index n, is defined in terms of its equivalent weight (EW), which is the mass of dry polymer (in grams) which contains 1 mol of sulfonate groups. Thus, for the Na salt of Nafion, Nafion EW = 866 refers to $n = 4$ and $m = 1$, Nafion EW = 966 is $n = 5$ and $m = 1$, Nafion EW = 1066 is $n = 6$, $m = 1$, and Nafion EW = 1166 is $n = 7$, $m = 1$. In this paper, we focus on Nafion EW = 1166. The hydrated Nafion can hold between 1 and 30 water molecules per SO_3 group. In the literature, the amount of water is specified by the weight percentage of water present (wt %). In these simulations we vary the water content from 3 to 20 H_2O per SO_3, corresponding to a variation between 5 and 19 wt % water, which roughly corresponds to a variation from 30% to 100% relative humidity.[21]

We use the AMBER force field FF02EP[17] in which the total energy is given by

$$E_{\text{tot}} = \frac{1}{2}\sum_{i,j} k_{ij}^{\text{bond}}(r_{ij} - r_0^{ij})^2 + \sum_i\sum_j\sum_k k_{ijk}^{\text{angle}}(\vartheta_{ijk} - \vartheta_0^{ijk})^2 + \frac{1}{2}\sum_i\sum_j\sum_k\sum_l\sum_n V_{ijkl}^{\text{dihedral}}(n)[1 + \cos(n\phi_{ijkl} - \gamma^{ijkl})] + \frac{1}{2}\sum_{i,j}\left[\frac{A}{r_{ij}^{12}} - \frac{B}{r_{ij}^{6}} + \frac{e^2 Z_i Z_j}{4\pi\epsilon_0\epsilon r_{ij}}\right] + E^{\text{pol}}(\{\alpha_i\}) \quad (2)$$

The first three terms give the harmonic potential energy of the chemical bonds, a harmonic energy of bending the angle defined by three atoms, and a harmonic energy for changing the dihedral angle defined by four atoms connected by three chemical bonds. Nonbonding interactions are represented by a sum of pairwise-additive Lennard-Jones 12−6 potentials. In addition, each atom has a charge and a static polarizability.

The FF02EP amber force field is a modified form of the FF99EP force field where the electrostatics of the test molecules are reevaluated at the B3LYP/cc-pVTZ/HF/6-31G* level of approximation.[17] The charges are fitted according to a RESP procedure[18] where the intramolecular self-polarization is explicitly included. The resulting force-field leads to minor modifications in the dihedral and van der Waals terms of the FF99EP potential set. The other terms are all obtained by fitting the potential energy surfaces, which in FF99 are calculated at either the MP2/6-31G* or MP4/6-31G* level of approximation.[19] Empirical rules provide the rest of the unknown parameters.

Certain interactions involving Nafion, which are not contained in the standard FF02EP force field, were taken from Table 1 of ref 10, while the interactions involving water were described by an unpolarizable, four-point, transferable intermolecular potential (TIP4P),[20] which is known to describe liquid water fairly accurately. Finally, we decided to include the effects of polarization because of the large electric fields likely to be present at such high ion concentrations. The polarizabilities used are those included in amber's FF02EP force field. Simulations that include polarizable water molecules are currently underway.

The structure of a polymeric system depends on the method of preparation, and it is rarely in a configuration corresponding to the lowest free energy; it is normally stuck in a local free energy minimum stabilized by the fact that to evolve to a lower minimum the chains will have to go through each other. Because of this, the stable configuration obtained in a simulation depends on the initial state of the system and on the fact that one cannot run the simulation for a sufficiently long time. Nevertheless, despite this limitation, we assume that we can learn something valuable about the nature of water and ion distribution in the hydrophilic channels by finding the most stable configuration compatible with a given type of initial state. The properties of the solution in the channels may not depend radically on the morphology of the domains.

When we start a simulation, we decide on a degree of hydration and the amount of Nafion present. We also need an initial configuration for the Nafion chains and the water. We have experimented with a cylindrical arrangement of the chains and with a configuration in which the Nafion chains form parallel plates. The water is inserted either inside the cylindrical pore or in the space between plates. The initial conformation of water is that of the bulk liquid, equilibrated at 300 K.

We prepare the state of the system as follows. All degrees of freedom, except for the bond lengths in the water and in the Nafion, are allowed to evolve. Bond constraints are enforced by using the SHAKE algorithm. This eliminates all high-frequency vibrations in the system and allows us to use a longer time step (0.001 ps). We run this preliminary simulation until the overall density of the swollen membrane becomes time independent. After that, we heat the system to 700 K and decrease the pressure from 1 to 0.2 bar and cool to 300 K twice at a pressure of 2 bar over the course of another 1 ns. After this preliminary preparation we start to collect data. We find that at the end of this "preparation" the system retains a memory of the initial configuration. A system that started as a planar "sandwich" evolves toward a planar (but rather corrugated) structure; the one that started as pores remain "fibrilar", but the cylindrical symmetry is destroyed. Regardless of the initial configuration, we run the molecular dynamics program at 300 K for 1−5 ns, using an NPT ensemble, to collect data. We are

TABLE 1: Equilibrium Properties of the Hydrated Nafion EW = 1166 Membranes[a]

wt % H_2O	ρ (g/cm^3)	$V/V_{5\ wt\ \%}$	H_2O/SO_3	RH (%)
5.0	1.830	1.000	3.4	25
7.0	1.743	1.098	7.3	66
19.0	1.688	1.245	14.5	98

[a] All properties are collected at 300 K and 1 atm pressure and averaged over 1 ns after the preliminary equilibration described in the text. Wt % H_2O is the weight percentage of water in the system. ρ is the mean density of the system (Nafion and water) in grams per cubic centimeter. The third column gives the volume of the simulation box divided by the volume occupied by Nafion with 5 wt % water. The fourth column gives the number of water molecules divided by the number of SO_3 groups. The last column reports the relative humidity needed for achieving the water loading given in the table (calculated from ref 22).

currently investigating in more detail to what extent the starting configuration affects water structure and dynamics within the hydrophilic channels. This paper is restricted to reporting results for the fibrillar structures.

III. Energetics in Hydrated Nafion EW = 1166

We have studied the properties of Nafion EW = 1166 for four levels of hydration. Table 1 shows that as the hydration increases from wt % = 5 to wt % =19% (~30%−100% relative humidity[21]), the polymer swells and its mean density decreases. This trend is in general agreement with what is known experimentally at 7.0 and 19.0 wt % hydration for the potassium salt of Nafion;[9] however, direct comparison is not possible since we have not found comparable data for the hydrated Na−Nafion membrane.

In Table 2 we show various mean electrostatic energies in the system, calculated after the system has equilibrated, as a function of the level of hydration. We explain the way we normalized these energies as we go along.

The first column of Table 2 gives the electrostatic interaction energy between Nafion chain and the sodium ion. The SO_3^- ion is included in the Nafion chain. Thus, the $Na^+-SO_3^-$ electrostatic interaction is a major factor in the chain−Na^+ interaction. However, this is not all: the potential energy includes some electrostatic charges on the Nafion backbone and on the side chains, and these contribute to the Nafion−Na^+ interaction. The Nafion−Na^+ interaction decreases with water loading. At low loading, there are not enough water molecules to solvate both Na^+ and SO_3^- and, as a result, these two ions are close together and interact strongly. We also observe a tendency of a Na^+ to bridge two SO_3^- ions. As the water content is increased, the dissociation of SO_3Na becomes more pronounced because both ions can be solvated. Thus, the Na^+ ion tends to drift into the water in the middle of the channel where it is solvated more completely. On the other hand, SO_3^- is tied to a side chain, which is hydrophobic. It is energetically unfavorable for the side chain to wander into the water, in the middle of the channel, because it would hinder the water−water interactions and break the network of hydrogen bonds. As a result, the side chains are "pushed" toward the border between the domain containing the polymeric backbone and the one containing water and drag the SO_3^- groups with them. Thus, the SO_3^- groups tend to be located at the border of the hydrophilic domain, so that they benefit from solvation but do not force the side chain into the aqueous medium. Because of all of these, the Na^+ ions find themselves inside the hydrophilic domain and the SO_3^- are at the domain's border. This increases the $Na^+-SO_3^-$ distance and is the main reason for the decrease of the Nafion−Na^+ electrostatic interaction energy. We emphasize that the numbers reported in the first column are the "bare" Coulomb interaction energies, which do not include the effect of water polarization, which screens the Coulomb interactions.

The second column shows a decrease of the Na^+-Na^+ electrostatic interaction energy with the addition of water. This happens because adding water allows a more complete hydration of the Na^+ ions, which leads to an increase of the distance between them.

The Nafion−Nafion electrostatic interaction is dominated by the repulsion between the SO_3^- groups. As water is added, the size of the hydrophilic domain increases. Since the hydrophobicity of the side chains forces the SO_3^- groups to reside near the border of the hydrophilic domain, increasing the "radius" of the domain tends to increase the distance between the SO_3^- groups and decrease the electrostatic interaction between them.

The fifth column gives the energy of the electrostatic interaction between Na^+ and water per sodium ion. Increasing the amount of water per ion increases the interaction energy. The same thing is seen in column six, which gives the electrostatic interaction between water and Nafion. This is dominated by the interaction of water with the SO_3^- groups, and the trend is the same as that seen for the Na^+−water interaction. However, the energy gained by the hydration of the SO_3^- groups is much smaller than that for the hydration of Na^+. There are two reasons for this. The first is a steric effect, where the side chain to which the SO_3 group is connected diminishes the space accessible to the water. The second factor is electrostatic: the charge on SO_3 is more diffuse than that on Na^+, and this diminishes the Coulomb interactions between the charges of water and those of SO_3^-.

The last column gives the water−water interaction energy per water molecule. For comparison we give, at the bottom of the column, the same quantity for bulk water (calculated with the potentials used here). Clearly, even at the highest hydration levels treated here the water is far from achieving a bulk structure. At low hydration level, each water molecule has few waters in its neighborhood (there are not enough molecules in

TABLE 2: Contributions to the Total Electrostatic Energy from the Na^+, H_2O, and Nafion Subsystems[a]

wt % H_2O	$\langle E_{Naf-Na^+}\rangle$ eV/ion	$E_{Na^+-Na^+}$ (eV/ion)	$\langle E_{Naf-Naf}\rangle$ eV/monomer	$\langle E_{Na-w}\rangle$ eV/ion	$\langle E_{Naf-w}\rangle$ eV/monomer	$\langle E_{w-w}\rangle$ eV/H_2O
5	−13.97	5.54	10.73	−2.28	−0.0485	−0.072
7	−10.66	3.96	9.58	−3.66	−0.395	−0.144
19	−9.14	2.66	8.78	−4.20	−1.004	−0.256
100						−0.434

[a] Here all average energies involving Nafion are for an individual monomer unit. $\langle E_{Naf-Na^+}\rangle$ is the total Nafion−Na^+ interaction energy divided by the number of Na^+ ions in the simulation cell, $\langle E_{Na^+-Na^+}\rangle$ is the total Na^+-Na^+ interaction energy divided by the number of Na ions in the simulation cell, $\langle E_{Naf-Naf}\rangle$ is the total Nafion−Nafion interaction energy divided by the number of Nafion monomer units in the simulation cell, $\langle E_{Na^+-w}\rangle$ is the total Na^+−water interaction energy divided by the number of Na^+ ions in the simulation cell, $\langle E_{Naf-w}\rangle$ is the total Nafion−water interaction energy divided by the number of Nafion monomer units, and $\langle E_{w-w}\rangle$ is the total water−water interaction energy divided by the number of water molecules in the simulation cell.

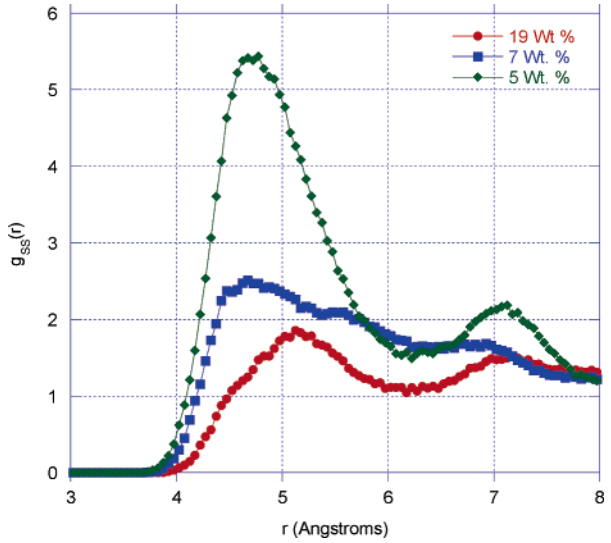

Figure 1. Calculated S−S radial distribution functions for Nafion EW = 1166 at different levels of hydration (reported in wt % water).

the domain, and their coordination is disrupted by the high concentration of ions).

IV. Structural Properties of the Material in the Hydrophilic Channels

IV.1. Introduction. The material in the hydrophilic domains forms an unusual state of matter, whose properties are determined by two factors. First, water is confined inside small pores, and second, the $-SO_3Na$ concentration in the hydrophilic channels is very high. The confinement disrupts the ability of water to create its normal, three-dimensional network of hydrogen bonds. In addition, the ion concentration is so large that practically every water molecule is engaged in ion hydration, and its structure is substantially different from that of bulk water. Finally, the number of water molecules per SO_3Na group determines the extent of the dissociation of SO_3Na into separated SO_3^- and Na^+ ions. At low water loading not all SO_3Na groups are ionized because there are not enough water molecules to solvate the ions and compensate for the Coulomb attraction between them.

These conditions combine to make the material inside the hydrophilic pores an interesting state of matter, whose properties are strongly dependent on the degree of hydration. We investigate here these properties by studying how the radial distribution functions, and the number of nearest neighbors of various constituents, depend on the amount of water. Additional information is gathered by examining the snapshots of the atomic positions in the simulations. In section IV.5.d. we calculate the structure factor that would be measured by inelastic neutron scattering from our system. Finally, in the last section we study the clustering of water in the hydrophilic channel and the onset of the percolation across the membrane.

IV.2. Properties of the SO_3 Groups. In Figure 1, we show how the sulfur−sulfur (S−S) radial distribution function (rdf) $g_{SS}(r)$ depends on the hydration level of the Nafion. In a system having 5 wt % water, $g_{SS}(r)$ has a large peak at $R = 4.6-4.7$ Å and a second peak at $R \sim 7.15$ Å. The origin of these peaks can be understood by examining the snapshot of the membrane hydrated to 5 wt %, shown in Figure 3.

The large peak occurs because, at 5 wt % hydration, there is insufficient water to create a large pore. This brings the SO_3Na in close proximity to each other. By examining snapshots of the simulations, we find that it is common for the Na ions to

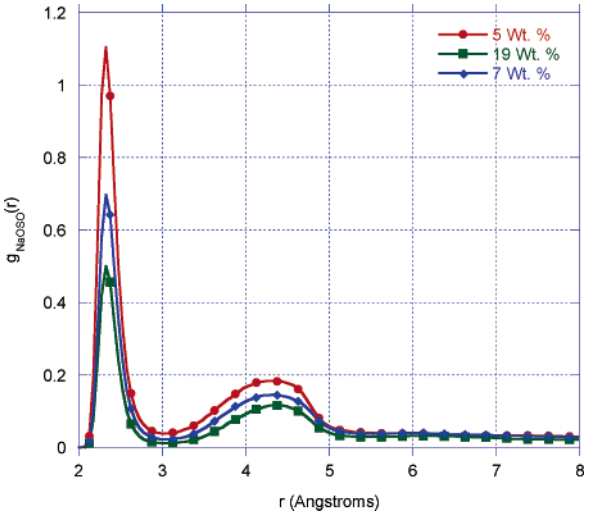

Figure 2. Na−OS radial distribution functions for the same systems. As the water content is increased, we see a decrease in the nearest-neighbor Na−OS peak, as the water effectively solvates the SO_3 headgroups and the Na ions move into solution, and a decrease in the nearest-neighbor S−S peak, as the membrane swells.

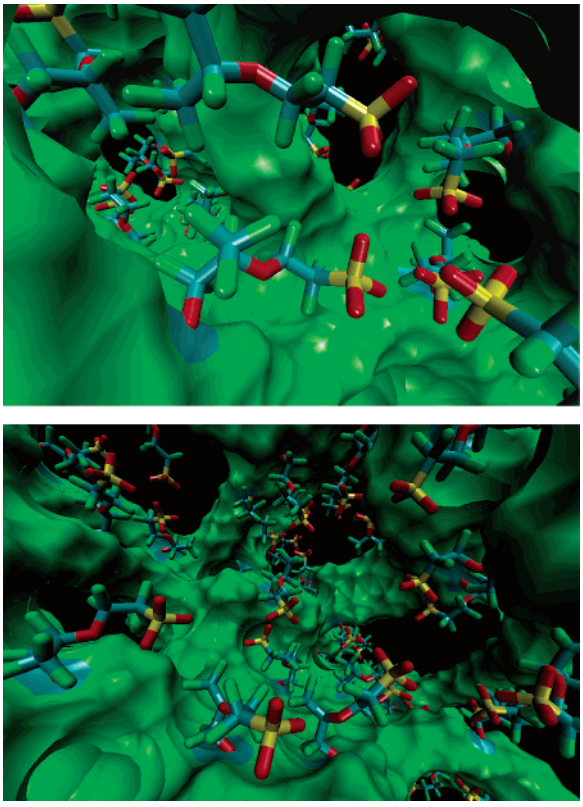

Figure 3. Snapshots of the Nafion structure in the channels of the hydrated membrane: (top) 5 wt % membrane; (bottom) 19 wt % membrane. The Teflon backbone is displayed as a surface while the sulfonate side chain is displayed explicitly. Oxygen is shown in red, carbon in gray, fluorine in green, and sulfur in yellow.

have two SO_3^- groups as nearest neighbors: the Na ion "cross-links" two SO_3^- groups across the pore, contributing to its small dimensions.

The second peak in $g_{SS}(r)$ at ~7.15 Å is likely to reflect the mean distance between the SO_3^- groups located on the opposite sides of the pore.

As the water content is increased, the peaks become less prominent, and a large number of S−S distances are present in the system. This reflects the fact that the pores are larger and

the SO_3^- groups tend to be located at the border between the hydrophilic and the hydrophobic domains.

Figure 2 shows the radial distribution function $g_{NaOS}(r)$ of the distance between Na^+ and an oxygen atom in the SO_3^- group. We pick this, rather than the Na−S distance, because Na^+ tends to coordinate with one of the oxygen atoms of the SO_3 group. $g_{NaOS}(r)$ has two peaks: one corresponds to Na^+ ions that are bound to SO_3^- and the other to dissociated (i.e., fully ionized) Na^+ ions. As water loading increases, the first peak becomes smaller and the second one grows. This peak evolution indicates that increase hydration causes more SO_3Na groups to dissociate and more Na^+ ions to move toward the middle of the pore.

IV.3. Conformation of the Side Chains in the Channels. Each hydrophobic side chain in Na−Nafion has a hydrophilic SO_3Na group at the end. We expect that the hydrophobic side chain is pushed out of the aqueous medium by the water molecules trying to make hydrogen bonds, while the SO_3Na, or the SO_3^- favors contact with water. As a compromise, the chains will lie along the border between the hydrophilic and the hydrophobic domains, with the SO_3Na group or the SO_3^- groups sticking out into the aqueous medium. This is in agreement with the observations of Gierke et al.[23] In Figure 3, we show snapshots of the side chains for a hydration of 5 and 19 wt %. In these figures, we render the Teflon backbone as a continuous surface, show the side chains explicitly, and hide the water and the Na. The figures show that the side chains hug the walls of the channel and the SO_3 groups are in contact with the hydrophilic medium.

IV.4.a. Na^+ Ions, Their Solvation, and Binding to SO_3^-. The $-SO_3Na$ group bound to the side chain is a strong electrolyte; given enough water, it will dissociate into ions. It is however not clear how this process proceeds in the hydrated Na−Nafion: there is a shortage of water, and full hydration cannot easily take place since the ions are confined to the hydrophilic channels and the ratio of ion to water is rather high (very high ion concentration in the water "solution").

As a consequence, the sodium ion is very likely to bridge several SO_3 groups, often across the channel. Furthermore, the sodium tends to surround itself with oxygen atoms, without much discrimination whether the oxygen is provided by SO_3 or water.

In this section, we examine the state of the Na atoms (or ions) by determining the number of SO_3 groups and of water molecules in the first "hydration" shell of the ion as a function of the water loading in the membrane.

Figure 4 shows histograms of the number of SO_3 groups in the first solvation shell of Na^+. An SO_3 group belongs to this shell if the center of one of its oxygen atoms is within 3.4 Å from the center of the sodium atom.

At the lowest hydration (5 wt %) only 11.5% of the Na atoms have no SO_3 group in the first solvation shell, which means that they are "fully ionized". 88.5% of all Na have at least one SO_3 group in the first solvation shell, with 16.5% of Na^+ having one sulfonate O, 34.5% having 2 sulfonate O, 32.5% having 3 sulfonate O, and 5% 4 sulfonate O (in the first solvation shell).

The fraction of Na atoms with no SO_3 in the first solvation shell increases steadily as the hydration level is increased. More interesting (and unexpected) is the fact that so many Na ions still have two or three SO_3 groups in the solvation shell. This is true even at the highest hydration level, though the fraction of such "cross-linking" decreases. When we used the same potential to examine a Nafion strand with a lot of water (98 wt % hydration), we found that sodium ions go in the solution and

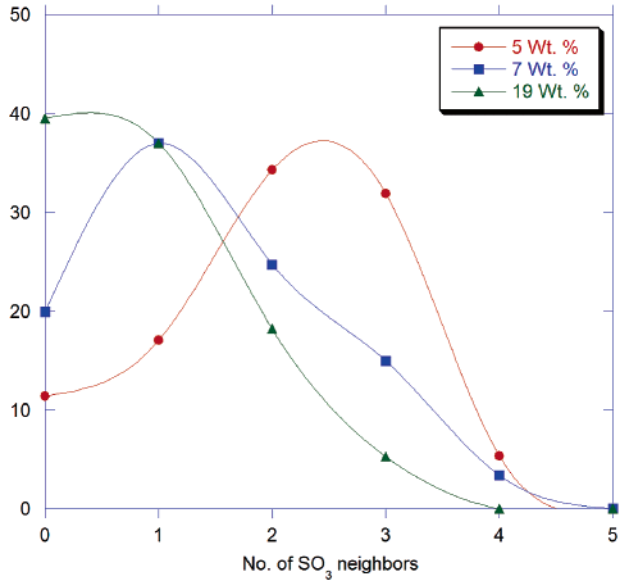

Figure 4. Histograms showing the number of SO_3 groups present in the first solvation shell of Na as a percentage of the total number of configurations measured. The lines are cubic-spline fits to the histogram data and are present only to guide the eye.

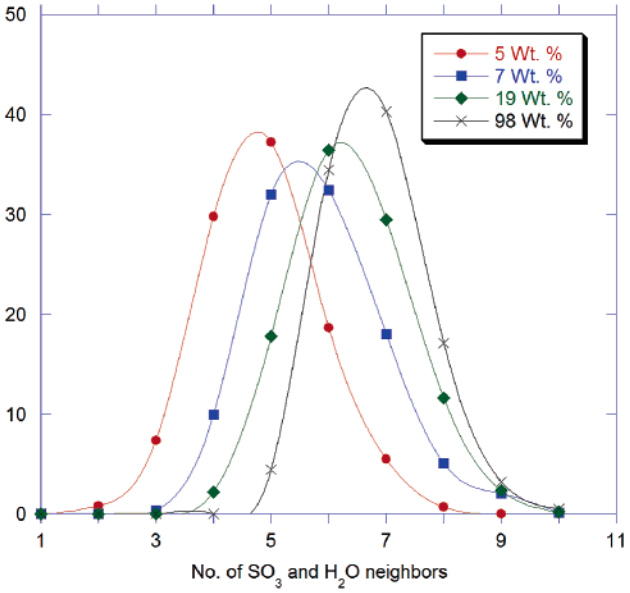

Figure 5. Histograms showing the total number of neighbors (SO_3 + H_2O) present in the first solvation shell of Na^+ as a percentage of the total number of configurations measured. The lines are cubic-spline fits to the histogram data and are present only to guide the eye.

are completely solvated. The fact that Na coordinates with several SO_3 groups is a consequence of the crowded conditions and high ion concentration in the hydrophilic domains, and it is not due to a bias in the potential energy.

We call the ability of sodium to "bind" to two or more SO_3 groups cross-linking. Sometimes cross-linking ties SO_3 groups that are along the domain wall, but there is a fair amount of cross-linking of SO_3 groups across the channel. This kind of cross-linking is qualitatively connected to the swelling observed upon hydration: the more the polymer swells, the fewer cross-channel cross-links it has. At 19 wt % hydration 76% of all Na ions do not cross-link. This decrease in cross-linking is accompanied by a steady increase in the number of water molecules present in the solvation shell.

IV.4.b. Na^+ Solvation by H_2O. In Figure 5, we show histograms that count the number of neighbors (SO_3 + H_2O)

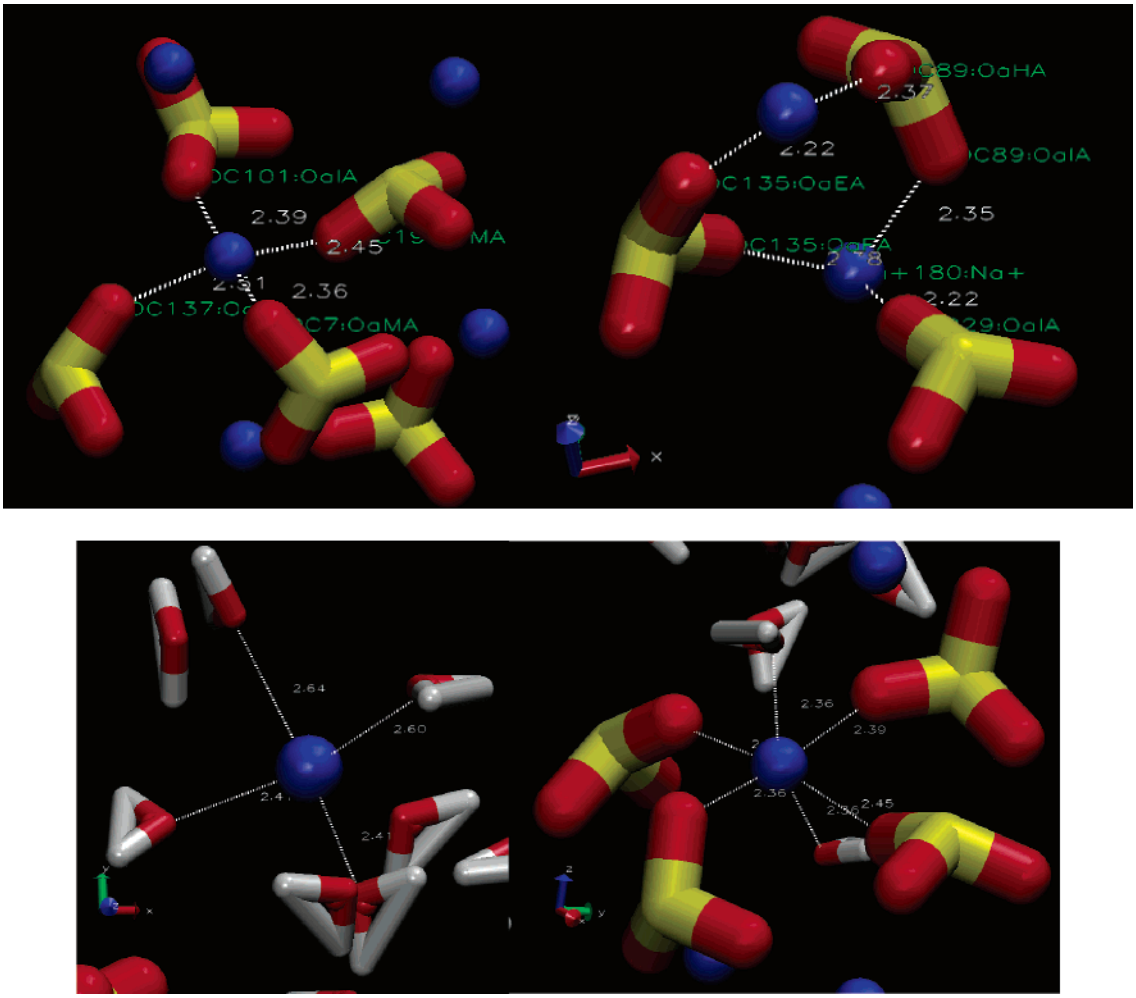

Figure 6. (a) Example configurations showing different Na^+ coordination environments at 5 wt % hydration: (left) a Na^+ ion cross-linking four different SO_3 groups; (right) two different Na^+ ions cross-linking two SO_3 groups and one cross-linking three SO_3 groups in the first solvation shell. Here O is in red, S in yellow, and Na^+ in blue. The dotted white lines denote the nearest neighbors, and their distances in angstroms are shown in white text. (b) Two Na^+ ion bonding environments at 5 wt % hydration: (left) a Na^+ ion with four water molecules and no SO_3 groups in the first solvation shell; (right) a Na^+ ion with four SO_3 groups and two H_2O in the first solvation shell. O is red, S is yellow, H is white, and Na is blue.

in the solvation shell of the sodium ions. We have chosen to present the number of H_2O and SO_3 molecules in one histogram because in both cases the Na ion coordinates with an oxygen atom in the two molecules. A comparison with Figure 4 allows a determination of the number of water molecules in the solvation shell of Na.

We compare the histograms at three hydration levels to the one obtained for 98 wt % hydration (1000 water molecules for every Na^+ ion). This high level of hydration cannot be achieved in a membrane; it corresponds to a Na−Nafion solution in water. In this system the Na^+ ion coordination with the oxygen atoms (from SO_3 or water) is similar to that seen in a NaCl(aq), with Na^+ forming a type of distorted octahedral cavity with 6−7 water molecules ordered around the ion. For all other water loadings studied here, the mean coordination of oxygen atoms around Na is less than in the 98 wt % solution and the histogram is broader, signaling a greater variation in the coordination from one Na atom to another.

For 5 wt % water loading, there are on average less than 4 oxygen atoms in the solvation shell of the Na^+ ion. Thus, the solvated Na^+ in 5 wt % Na−Nafion differs substantially from that in aqueous NaCl. Snapshots of typical bonding environments are shown in Figure 6. As the hydration increases, we see a gradual increase of the number of water molecules and of the total number of oxygen atoms in the first hydration shell. At 7 wt % we have roughly 4−5 water molecules as nearest neighbors. At a 19 wt % this increases to roughly 5−6, and the mean number of oxygen atoms is around 7. In this case the solvation around sodium is similar to that seen in aqueous NaCl-(aq) solution, with some of the water O replaced by an O atom from an SO_3 group.

IV.5. Water Structure. The hydrophilic domains are interesting in that they are small in cross section and possess extremely high concentrations of ions. These factors are likely to force water into an unusual structure that differs from that generally seen in bulk water. To illustrate this difference, we examine the water structure in the hydrophilic domain.

IV.5.a. Water−Water Hydrogen-Bonding Networks. We say that two water molecules are neighbors when an oxygen atom from one molecule is less than 3.5 Å away from an oxygen atom from the other molecule. In Figure 7, we show histograms of the number of water molecules coordinated with a given water, collected from a large number of molecules, at many different times during the simulation. At 5 wt % hydration each water molecule has, on average, two waters in its "first shell", while at 7 wt % water there are three neighbors. Even in the 19 wt % system, where we see a significant number of 4-fold-coordinated water molecules, we do not reach the coordination seen in bulk water. The distribution of the number of water neighbors of a water molecule is significantly broader in the

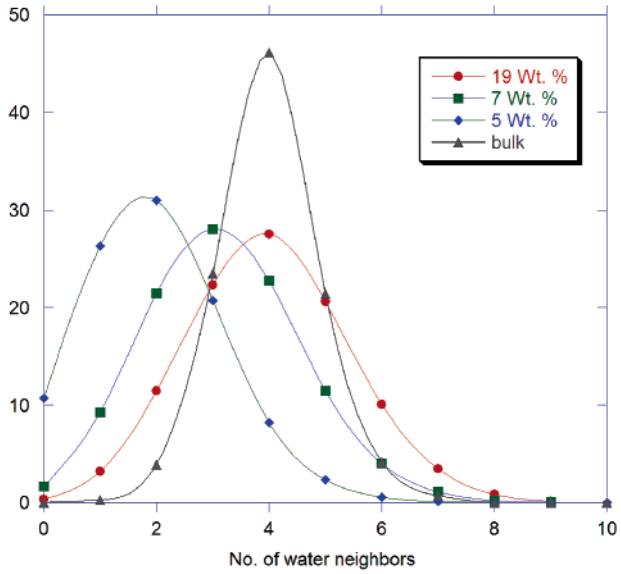

Figure 7. Histogram showing the percentage of H_2O that have a specific number of neighboring H_2O. The different curves correspond different levels of hydrated Nafion along with the result for bulk water. Here the nearest neighbors are defined as those water O that are with 3.2 Å of one another. The lines have no physical meaning and are only there to guide the eye between the points. A linear scale is used for the both the ordinate and the abscissa.

Nafion than in bulk water. This is reasonable; the water molecules located at the border between the two domains and the water solvating the ions have fewer water molecules as neighbors than the bulk water. However, surprisingly, we also see that some water molecules in Nafion have eight water neighbors, a situation we do not find in the bulk water. By examining many pictures, we found that such highly coordinated water molecules are located in the overlapping, second solvation shells of two Na ions. An example of such a configuration is shown in Figure 8.

IV.5.b. Water Cluster Size. The continuity of the hydrophilic domains, from one side of the membrane to another, is necessary for ion transport across the membrane. A channel that does not provide a continuous water pathway across the membrane cannot contribute to the electrochemistry that generates the current in the fuel cell. For this reason, we examine the ability of the water molecules to form percolating clusters, as a function of the hydration level.

The cluster size in a simulation is determined by starting with a given water molecule and checking whether its oxygen atom has an oxygen atom from another water molecule within 3.5 Å. A water molecule whose oxygen atom is within this sphere belongs (by definition) to the same cluster as the initial molecule. Next, we check whether the second molecule has another water molecule within 3.5 Å, etc. This search stops when the procedure does not add a new molecule to the cluster. Then, we initialize a new cluster by starting with a molecule that is not part of any of the clusters already identified. We repeat this process until we have examined all water molecules.

We show the size distribution of the water clusters defined in this way in Figure 9. In a membrane with 5 wt % water, 50% of the water molecules form clusters of 10 or less and the remaining 50% are in clusters of 10−40 water molecules. We conclude that at this low level of hydration the hydrophilic channels consist of "droplets" separated by hydrophobic material. Since the distance between clusters is at least 3.5 Å and since the proton mass is substantial, we expect that proton tunneling from one cluster to another is extremely slow. Proton

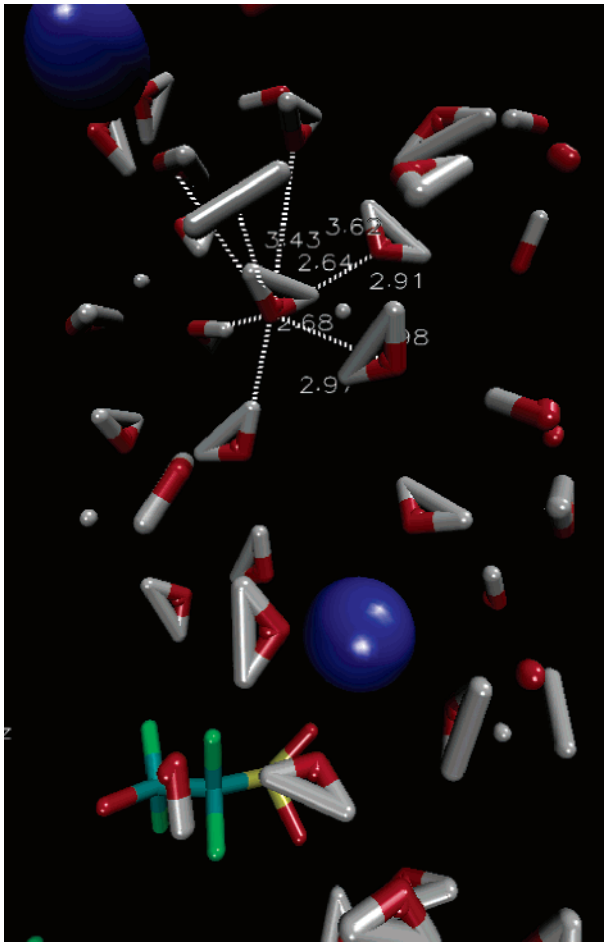

Figure 8. A snapshot showing a water with a large number of water neighbors. In this figure, O is in red, H in gray, F in green, and C in green/blue, and Na are the large blue spheres. The dotted white lines show the distances to neighbor water O along with their distance in angstroms.

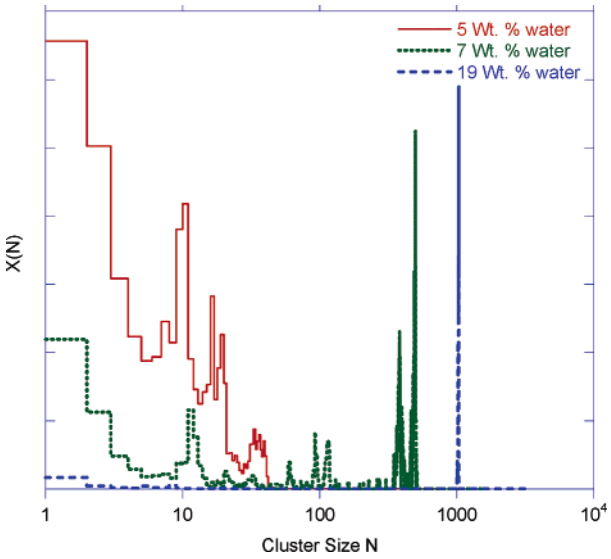

Figure 9. Apparent cluster size distribution, N, for the unit cell plotted as $X(N) = N \times$ (frequency of occurrence). Note that the vertical scale for the 19 wt % Nafion has been divided by 5 for ease of viewing and that clusters in excess of 87 water molecules can potentially percolate throughout the membrane.

conductivity may take place, however, if a structural fluctuation brings clusters closer to each other. However, since such fluctuations are likely to be rare, their contribution to conductiv-

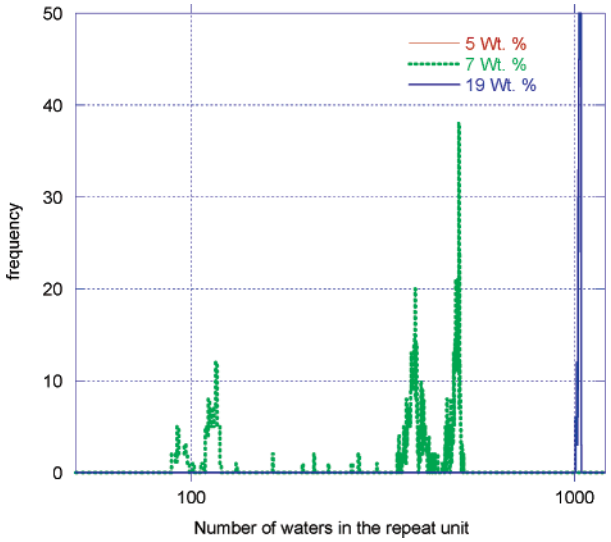

Figure 10. A histogram of the number of waters that aggregate and form percolated channels throughout the membrane.

ity is small. There may also be contributions to conductivity due to variations in the size of the hydrophilic channels from one region of the membrane to another. Even if the *mean* hydration is 5 wt %, this does not preclude having in the system some channels with a higher local hydration level, formed accidentally during membrane preparation. Such channels will have higher conductivity than expected on the basis of the mean hydration level.

A slight increase of the hydration level to 7 wt % brings about a dramatic shift in the cluster size distribution. Now clusters with several hundred water molecules are common, but some small clusters still exist in the system. At 19 wt % water most clusters have 1000 molecules, but a few maverick molecules form very small clusters. These are probably stuck in some fold of the channel wall.

IV.5.c. Water Percolation through the Channels. Because we apply periodic boundary conditions in all directions, including the direction along the hydrophilic tube, the cluster size is misleading if a cluster percolates through the membrane; in this case, the true cluster size is of the order of membrane thickness. With the cluster-defining algorithm used here, we know that a cluster percolates through the whole pore if it includes a periodic image of one of cluster's molecules. We have used this algorithm to determine whether the system contains percolating clusters. In Figure 10 we present a histogram of the clusters that percolate through our simulation box.

At 5 wt % no percolation structures were found over the duration of the simulation (this is why there are no results for 5 wt % loading in Figure 10). In this case, the water in the hydrophilic channels forms a series of narrow, winding, discontinuous, irregular clusters and isolated droplets—that may connect to one another via temporary water bridges. This finding agrees with the earlier work of Vishnyakov and Neimark[9] and the later work of Jang et al.[2] The figure shows that percolation clusters are present at a loading of 7 wt %. In some cases, we find clusters that have less than 100 molecules but manage to go from one end of the simulation box to another. This means that such clusters are very narrow, almost one-dimensional. Of course, even though such a thin cluster goes from one end of the simulation box to the other, we do not expect them to extend through the whole membrane. It is however possible that clusters percolating through the membrane have, occasionally, such thin "necks". It is difficult to estimate the effect of such "necks" on proton diffusion.

As we increase the level of hydration, we see an increasing tendency for the water molecules to form percolating networks throughout the membrane. At 7 wt % hydration, 90% of the water is engaged in a percolating network. This figure jumps to 99% at 19 wt % hydration. This happens because the energy favors overwhelmingly the formation of a concentrated ionic solution in water and wins over the tendency of entropy to spread the molecules in as large a space as possible. Water−water interactions are fairly strong; in addition, the presence of the ions and their solvation favors the formation of a continuous water-ion phase. Given these, percolation is likely to take place whenever the system has enough water.

In Figure 11 we show the hydrophilic phase of Nafion with 19 wt % water, which shows that the hydrophilic phase is continuous and has an irregular shape. This is in agreement with the dissipative particle dynamics calculations of Yamamoto and Hyodo.[11]

IV.5.d. Small-Angle Neutron Scattering (SANS). The small-angle scattering profile of the hydrated Nafion membrane has a single, broad feature known as the "ionomer peak".[24,25] Many models were proposed for explaining these data: the cluster−network model of Gierke et al.,[23,26,27] the core−shell model of Fujimura et al.,[28,29] the local-order model of Dreyfus and co-workers,[30,31] the lamellar model of Litt,[32] the sandwich model,[25] the fibrillar model of Rubatat et al.,[33−35] and the connected rod network model of Gebel and Moore.[24] All of them assume that the ionic groups aggregate to form a network of clusters. In our simulations we started with a configuration that most closely resembles the fibrillar model of Rubatat et al. and the rodlike model of Gebel and Moore.[24,33−35] We have also performed simulations that start with a sandwich-like configuration that more closely resemble the models of Haubold et al.[25] or Litt.[32]

To connect the structure produced by our simulation with the neutron scattering data, we calculate the structure factor

$$S(\vec{q}) = \langle \sum_i \sum_j (\delta_i - \langle\delta\rangle)(\delta_j - \langle\delta\rangle) e^{i\vec{q}\cdot\vec{r}_{ij}} \rangle / L^3 \qquad (3)$$

Here $(\delta_i - \langle\delta\rangle)$ is the contrast, which is a measure of the difference in the scattering length of the medium of interest δ_i and that of the surrounding medium $\langle\delta\rangle$. For SANS this is the contrast in the neutron scattering length, and for small-angle X-ray scattering (SAXS), it is the contrast in the X-ray scattering factors for the appropriate elements. The angular brackets denote an ensemble average. We have calculated the spherically averaged structure factor $S(q)$ as[2]

$$S(|\vec{q}|) = \sum_{|\vec{q}|} S(\vec{q}) / \sum_{|\vec{q}|} 1 \qquad (4)$$

This accounts for the fact that the domain simulated will, in general, have no preferred orientation with respect to the incoming neutrons. This average was performed by molecular dynamics, in a run of over 0.5 ns.

The results are shown in Figure 12. The simulations predict large changes in the SANS profile as a function of hydration. The formation of a bicontinuous phase is characterized by a narrowing of the SANS profile. At high hydration, the observed profile is qualitatively in agreement with what is found experimentally except that the peak in our case is at 0.16 $Å^{-1}$ while in experiments it is at 0.13 $Å^{-1}$. A possible reason for this difference is the small unit cell used in simulations. This agreement is interesting since the morphology of the hydrophilic phase in our simulations is quite different from the network−cluster model proposed by Gierke et al.[23,26,27] in their interpreta-

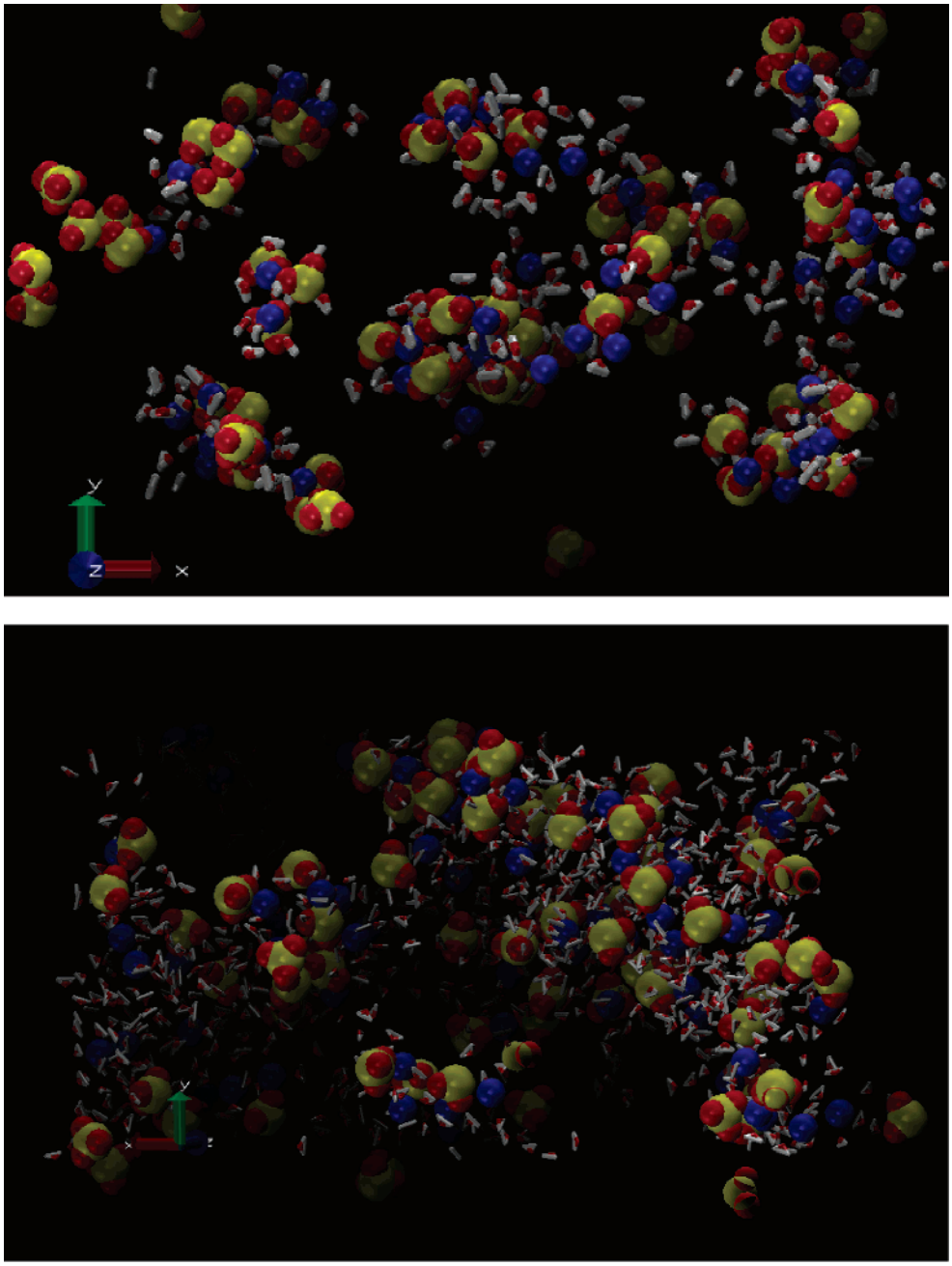

Figure 11. **(**top) A snapshot of the water channels in a simulated Nafion (Dupont) membrane hydrated to 5 wt % with water. (bottom) A snapshot of the water channels in a simulated Nafion (Dupont) membrane hydrated to 19 wt % with water. For ease of viewing we show only the hydrophilic subphase with S in yellow, O in red, Na^+ in blue, and H in white.

tion of SAXS experiments. Visually, the hydrophilic domains are consistent with the basic tenets of the local-order models, the fibrillar model,[35] the sandwich structure model, and the connected rod network model of Gebel and Moore.[24]

At lower hydration levels one sees a "broadening" of the profile —presumably reflecting the inhomogeneity in water "cluster" distributions. The 5 wt % membrane has a calculated profile that resembles that seen of room humidity for the EW 800 perfluorinated sulfonate ionomer.[24]

V. Conclusions

We have investigated the structural properties of the hydrophilic phase, by using molecular dynamics, as a function of the hydration level. We have shown that the main factors controlling the structure of the system are the hydration energies and the electrostatic interactions. The elasticity of the Teflon chains and the water−water interaction seem to be less of a determining factor. At 5 wt % hydration we find that the hydrophilic domains are disjoint, and they can be loosely described as droplets that do not form a continuous cluster across the membrane. In this case there are not enough water molecule to solvate the ions and most of the $-SO_3H$ groups are not dissociated. As the amount of water in the membrane is increased, the ions become more effectively solvated, and the strain on the Nafion introduced by aggregation of the sulfonate headgroups is relieved by membrane swelling. The charges are screened by the water, and a transition to a percolating channel network is seen for the hydrophilic phase. Now the water forms irregular curvilinear channels that make continuous paths in all directions. For 19 wt % water these channels have dimensions of the order of 10−20 Å in cross section. Despite the fact that the morphology bears little resemblance to the cluster−network

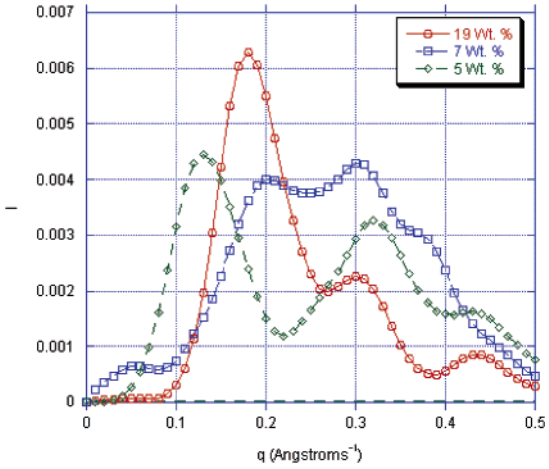

Figure 12. Calculated $S(q)$ ($T = 300$ K, $P = 1$ atm) for hydrated Nafion. The three curves correspond to structure factors obtained with 5, 7, and 19 wt % water present in the membrane. Each profile was obtained as a configurational average of 500 shapshots of the periodic system recorded over 0.5 ns.

model[23,26,27,36] or the core−shell model of Fujimura et al.[28,29] (invoked in attempts to explain the results of X-ray or neutron scattering experiments), our percolating structure gives a scattering profile that qualitatively agrees with experiment. Visually the hydrophilic domains appear to be consistent with the basic tenets of the local-order models, the fibrillar model,[35] the sandwich structure model,[25] and the connected-rod network model of Gebel and Moore.[24] At 5 wt % water the "channels" and droplet dimensions are of the order of 5−8 Å.

At all levels of hydration the pendant perfluorovinyl side chains in the Nafion hug the walls of the channel, because in doing so they allow an increase of the water−water interaction. The sulfonate groups point into the hydrophilic phase to increase the degree of solvation of $-SO_3^-$. At 5 wt % water hydration Na^+ ions may have several $-SO_3^-$ groups in their first solvation shell, and there is insufficient water present to fully solvate the ions. Consequently, the Na ions have on average of three oxygen atoms from water and two from the SO_3 group in their first solvation shell. As the water level is increased, we see the formation of an octahedral solvation shell around the Na^+ ions composed of either oxygen atoms from water or SO_3^-. The higher the hydration level, the more H_2O are to be found in this first solvation shell. The high ion concentration, coupled with the dominance of H_2O−ion interactions over H_2O-H_2O interactions, prevents the formation of a tetrahedrally coordinated water network. At 5 wt % hydration, on average, each water has only two water molecules in its neighborhood, while at 7 wt % water there are three such neighbors. Even in the 19 wt % system, where we see the establishment of a 4-fold-coordinated water network, a comparison with bulk water indicates that the distribution of the number of water neighbors (around a water molecule) is significantly broader in the Nafion. For water molecules that lie near the walls of the domain or are next to a Na ion, one can expect fewer H_2O neighbors, while for water molecules that reside in the second solvation shell of two or more ions, one can find much higher numbers of water neighbors—sometimes as high as 8−10.

Acknowledgment. This work was supported by a MURI grant from the US Army Research Office.

References and Notes

(1) Paddison, S. J. *Annu. Rev. Mater. Res.* **2003**, *33*, 289.
(2) Jang, S. S.; Molinero, V.; Cagin, T.; Goddard, W. A. *J. Phys. Chem. B* **2004**, *108*, 3149.
(3) Jinnouchi, R.; Okazaki, K. *J. Electrochem. Soc.* **2003**, *150*, E66.
(4) Li, T.; Wlaschin, A.; Balbuena, P. B. *Ind. Eng. Chem. Res.* **2001**, *40*, 4789.
(5) Paddison, S. J.; Zawodzinski, T. A. *Solid State Ionics* **1998**, *115*, 333.
(6) Rivin, D.; Meermeier, G.; Schneider, N. S.; Vishnyakov, A.; Neimark, A. V. *J. Phys. Chem. B* **2004**, *108*, 8900.
(7) Spohr, E. *Mol. Simul.* **2004**, *30*, 107.
(8) Vishnyakov, A.; Neimark, A. V. *J. Phys. Chem. B* **2000**, *104*, 4471.
(9) Vishnyakov, A.; Neimark, A. V. *J. Phys. Chem. B* **2001**, *105*, 9586.
(10) Vishnyakov, A.; Neimark, A. V. *J. Phys. Chem. B* **2001**, *105*, 7830.
(11) Yamamoto, S.; Hyodo, S. A. *Polym. J.* **2003**, *35*, 519.
(12) Ioselevich, A. S.; Kornyshev, A. A.; Steinke, J. H. G. *J. Phys. Chem. B* **2004**, *108*, 11953.
(13) Hayashi, H.; Yamamoto, S.; Hyodo, S. A. *Int. J. Mod. Phys. B* **2003**, *17*, 135.
(14) Elliott, J. A.; Hanna, S.; Elliott, A. M. S.; Cooley, G. E. *Phys. Chem. Chem. Phys.* **1999**, *1*, 4855.
(15) Dyakov, Y. A.; Tovbin, Y. K. *Russ. Chem. Bull.* **1995**, *44*, 1186.
(16) Petersen, M. K.; Wang, F.; Blake, N. P.; Metiu, H.; Voth, G. A. *J. Phys. Chem. B* **2005**, *109*, 3727.
(17) Cieplak, P.; Caldwell, J.; Kollman, P. *J. Comput. Chem.* **2001**, *22*, 1048.
(18) Cornell, W. D.; Cieplak, P.; Bayly, C. I.; Kollman, P. A. *J. Am. Chem. Soc.* **1993**, *115*, 9620.
(19) Wang, J. M.; Wolf, R. M.; Caldwell, J. W.; Kollman, P. A.; Case, D. A. *J. Comput. Chem.* **2004**, *25*, 1157.
(20) Jorgensen, W. L.; Chandrasekhar, J.; Madura, J. D.; Impey, R. W.; Klein, M. L. *J. Chem. Phys.* **1983**, *79*, 926.
(21) James, P. J.; Elliott, J. A.; McMaster, T. J.; Newton, J. M.; Elliott, A. M. S.; Hanna, S.; Miles, M. J. *J. Mater. Sci.* **2000**, *35*, 5111.
(22) Elliott, J. A.; Hanna, S.; Elliott, A. M. S.; Cooley, G. E. *Macromolecules* **2000**, *33*, 4161.
(23) Gierke, T. D.; Munn, G. E.; Wilson, F. C. *J. Polym. Sci., Part B* **1981**, *19*, 1687.
(24) Gebel, G.; Moore, R. B. *Macromolecules* **2000**, *33*, 4850.
(25) Haubold, H. G.; Vad, T.; Jungbluth, H.; Hiller, P. *Electrochim. Acta* **2001**, *46*, 1559.
(26) Gierke, T. D. *J. Electrochem. Soc.* **1978**, *125*, C163.
(27) Gierke, T. D. *Bull. Am. Phys. Soc.* **1981**, *26*, 462.
(28) Fujimura, M.; Hashimoto, T.; Kawai, H. *Macromolecules* **1981**, *14*, 1309.
(29) Fujimura, M.; Hashimoto, T.; Kawai, H. *Macromolecules* **1982**, *15*, 136.
(30) Aldebert, P.; Dreyfus, B.; Gebel, G.; Nakamura, N.; Pineri, M.; Volino, F. *J. Phys. (Paris)* **1988**, *49*, 2101.
(31) Dreyfus, B.; Gebel, G.; Aldebert, P.; Pineri, M.; Escoubes, M.; Thomas, M. *J. Phys. (Paris)* **1990**, *51*, 1341.
(32) Litt, M. H. *Polym. Prepr.* **1997**, *38*, 80.
(33) Rubatat, L.; Rollet, A. L.; Diat, O.; Gebel, G. *J. Phys. IV* **2002**, *12*, 197.
(34) Rubatat, L.; Rollet, A. L.; Gebel, G.; Diat, O. *Macromolecules* **2002**, *35*, 4050.
(35) Rubatat, L.; Gebel, G.; Diat, O. *Macromolecules* **2004**, *37*, 7772.
(36) Gierke, T. D. *J. Electrochem. Soc.* **1977**, *124*, C319.